Eco-Cooperative Adaptive Cruise Control at Signalized Intersections Considering Queue Effects

Hao Yang, Hesham Rakha, *Member, IEEE*, and Mani Venkat Ala

***Abstract*— Traffic signals typically introduce vehicle stops along a trip and thus increase vehicle fuel consumption levels. In attempt to enhance vehicle fuel efficiency, eco-cooperative adaptive cruise control (Eco-CACC) systems are being developed that receive signal phasing and timing data from downstream signalized intersections via vehicle-to-infrastructure communication. In this paper, an Eco-CACC algorithm is developed that computes the fuel-optimum vehicle trajectory through a signalized intersection by ensuring that the vehicle arrives at the intersection stop bar just as the last queued vehicle is discharged. A simulation analysis demonstrates that the proposed Eco-CACC system produces vehicle fuel savings up to 40%, when the market penetration rate (MPR) is 100%. The results also demonstrate that for single-lane approaches, the algorithm reduces the overall fuel consumption levels for all vehicles, and that higher MPRs result in larger savings. Alternatively, on multi-lane approaches, lower MPRs produce negative impacts on the overall intersection fuel efficiency, and only when MPRs are greater than 30% does the algorithm produce overall intersection fuel consumption savings.**

***Index Terms*— Eco-CACC, connected vehicles, automated vehicles, advisory speed limits, vehicle fuel consumption, queue length prediction.**

I. Introduction

In THE last two decades, the transportation system has resulted in increased energy usage and air pollutant emissions. In the U.S. alone, the transportation sector consumed over 135 billion gallons of fuel in 2013, and more than 70% was consumed by passenger cars and trucks [1]. Globally, 60% of the oil consumption is consumed by the transportation sector [2]. The urgent need to reduce the transportation sector fuel consumption levels requires researchers and policy makers to develop various advanced fuel-reduction strategies. Eco-driving is one efficient and cost effective strategy to improve the fuel efficiency of the transportation sector [2]. The major idea behind eco-driving is providing real-time driving advice to individual vehicles so that the drivers can adjust their driving behavior or take driving actions to reduce fuel consumption and emission levels. Generally, most eco-driving strategies are operated by providing real-time driving advice, such as advisory speed limits, recommended acceleration and/or deceleration levels, speed alerts, etc. To date, numerous studies have indicated that eco-driving can reduce fuel consumption and greenhouse gas (GHG) emissions by approximately 10% on average [3].

The major causes of high fuel consumption levels and air pollutant emissions generated by vehicles have been widely investigated. Frequent accelerations associated with stop-and-go waves [4], [5], excessive speeds over 60 mph, slow movements on congested roads [5], [6], and extra idling times are major causes of increased vehicle fuel consumption and emission levels. Consequently, it is clear that reducing traffic oscillations and avoiding idling are two critical ways to reduce fuel consumption levels.

In general, eco-driving research can be categorized as freeway-based and city-based strategies. On freeways, the traffic stream is continuous; and vehicles are rarely disturbed by traffic control devices, i.e., a vehicle can travel to a particular destination without any extra constraints (except for turbulence caused by on- and off-ramps). Developing eco-driving strategies on freeways is relatively straightforward. The strategies compute advisory speeds or speed limits for drivers based on road traffic conditions, and alter driving behavior to minimize vehicle fuel consumption and emission levels. Barth and Boriboonsomsin utilized vehicle-to-infrastructure (V2I) communication to gather average link speed and variance statistics, and to provide advisory speeds to drivers to reduce emissions and fuel consumption levels [7]. Yang and Jin estimated advisory speed limits based on the movements of surrounding vehicles with the assistance of vehicle-to-vehicle communications [8]. Ahn and Rakha developed a moving-horizon dynamic programming Eco-Adaptive Cruise Control (Eco-ACC) system and demonstrated its potential benefits [9]–[11].

Unlike freeways, traffic stream motion along arterial roads is typically interrupted by traffic control devices. Vehicles are forced to stop ahead of traffic signals when encoun-

Manuscript received March 5, 2016; revised July 17, 2016 and August 30, 2016; accepted September 17, 2016. Date of publication October 13, 2016; date of current version May 29, 2017. This work was supported in part by the TranLIVE University Transportation Center and in part by the Connected Vehicle Initiative University Transportation Center. The Associate Editor for this paper was S. Siri.

H. Yang is with the Department of Civil and Environmental Engineering, Lamar University, Beaumont, TX 77710 USA (e-mail: hyang1@lamar.edu).

H. Rakha is with the Charles E. Via, Jr. Department of Civil and Environmental Engineering, Virginia Tech Transportation Institute, Virginia Polytechnic Institute and State University, Blacksburg, VA 24061 USA (e-mail: hrakha@vtti.vt.edu).

M. V. Ala is with KLD and Associates, Ltd., Islandia, NY 11749 USA (e-mail: amvsk@vt.edu).

Color versions of one or more of the figures in this paper are available online at http://ieeexplore.ieee.org.

Digital Object Identifier 10.1109/TITS.2016.2613740

tering red indications, producing shock waves within the traffic stream. These shock waves in turn result in vehicle acceleration/deceleration maneuvers and idling events, which increase vehicle fuel consumption and emission levels. Most research efforts have focused on optimizing traffic signal timings using traffic arrival rates and vehicular queue lengths [12], [13]. Recently, with the development of connected vehicles (CVs), individual vehicles can be controlled to minimize emissions and fuel consumption levels. The CVs enable vehicles to exchange road traffic information, and to communicate with traffic signal controllers to receive SPaT information [14]. These information can be applied to estimate fuel-optimum trajectories for vehicles to travel on arterial roads.

In the past decade, environmental CV applications have attracted significant research interests. Most of these efforts assist drivers in their travel along signalized intersections by providing fuel-optimum trajectories. Mandava et al. and Xia et al. proposed a velocity planning algorithm based on traffic signal information to maximize the probability of encountering a green indication when approaching multiple intersections [15], [16]. The algorithm attempted to reduce fuel consumption levels by minimizing acceleration/deceleration levels while avoiding complete stops. It should be noted, however, that lowering acceleration/deceleration levels does not necessarily imply reducing fuel consumption levels. Asadi and Vahidi applied traffic signal information to design optimal cruise speeds for probe vehicles to minimize the probability of stopping at signals during red indications [17]. Malakorn and Park utilized SPaT information and developed a cooperative adaptive cruise control system to minimize absolute acceleration levels of probe vehicles [18]. Barth et al. developed a dynamic eco-driving system for arterial roads, which computes optimum acceleration/deceleration profiles for probe vehicles to minimize the total tractive power demand and the idling time so that the fuel consumption levels were reduced [19]. Rakha and Kamalanathsharma constructed a dynamic programming based fuel-optimization strategy using recursive path-finding principles, and evaluated it with an agent-based model [20]–[22]. De Nunzio et al. used a combination of a pruning algorithm and an optimal control to find the best possible green wave if the vehicles were to receive SPaT information from multiple upcoming intersections [23]. In addition, Green Light Optimized Speed Advisory (GLOSA) systems, which utilize vehicle-to-infrastructure communications, have been widely investigated to assist drivers in traversing intersections efficiently. The GLOSA systems estimate optimal advisory speeds for individual vehicles proceeding through single and multiple traffic signals to minimize delay and fuel consumption levels [24]–[27]. In Europe, the eCoMove project [28] applied CVs to combine green trip planning and route choice algorithms with eco-driving strategies in urban areas, and the integrated system saved overall fuel consumption and GHG emissions by as high as 10%. Furthermore, various smartphone applications have been developed to realize eco-driving assistant systems for vehicles in the vicinity of signalized intersections [29], [30].

Most existing studies related to eco-driving on arterial corridors attempt to minimize idling time and smooth acceleration/deceleration maneuvers without considering the impact of surrounding traffic. However, in reality, the idling events are determined not only by the SPaT information, but also by vehicle queues at signalized intersection approaches. While, this problem is rarely studied in the literature. References [31] and [32] applied micro-simulations to evaluate the effectiveness of eco-driving with moderate acceleration/deceration during queue discharge. References [33] and [34] estimated optimal speed profiles for individual vehicles with the consideration of vehicle queues and road grade conditions. However, these studies do not integrate the queue estimation into the algorithm, which makes them difficult to be applied in real-time applications. Moreover, most research efforts focus on optimizing speed profiles of equipped vehicles upstream of the intersection but ignore the acceleration behavior downstream of the intersection after the traffic signal turns green, which results in more fuel usage of vehicles proceeding through intersections. In this paper, we conduct a comprehensive analysis of eco-CACC systems on arterial roads to fill this gap. We first investigate the impact of the SPaT and the vehicle queue information on fuel consumption levels at signalized intersections. Then, the impact of vehicle queues on the Eco-CACC algorithm proposed in [22], in which vehicle queue information is not used, is analytically investigated. Based on the analysis, an Eco-CACC algorithm with the consideration of vehicle queue estimation is developed to minimize fuel consumption levels. We also evaluate the benefits of the algorithm within a microscopic simulation environment, and evaluate the impact of market penetration rates of probe vehicles and intersection configurations on the system performance.

In terms of the paper layout, Section II introduces a kinematic wave model to describe the generation and release of vehicle queues and to estimate queue lengths. Section III describes the development of the proposed Eco-CACC algorithm with the consideration of vehicle queues. Section IV evaluates the energy and environmental benefits of the algorithm using microscopic simulations. Finally, Section V summarizes the study conclusions.

II. Queue Estimation at Intersections

This paper attempts to develop an Eco-CACC algorithm that predicts vehicle queues upstream of a signalized intersection to develop fuel-optimum vehicle trajectories in the vicinity of signalized intersection. In this section, a kinematic wave model is first reviewed to describe traffic dynamics on a signalized road, and is used to predict the vehicle queue length.

The Lighthill-Whitham-Richard (LWR) [35], [36] is one traditional kinematic wave model that describes traffic dynamics on roads. Assume that $\{\rho(x,t), v(x,t), q(x,t)\}$ represent the density, speed, and flow at location x and time t, respectively then the LWR model gives

$$\frac{\partial \rho(x,t)}{\partial t} + \frac{\partial q(x,t)}{\partial x} = 0. \tag{1}$$

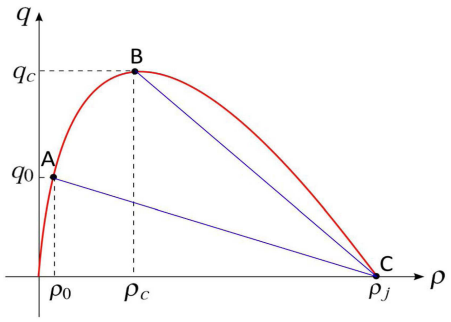

Fig. 1. Fundamental Diagram.

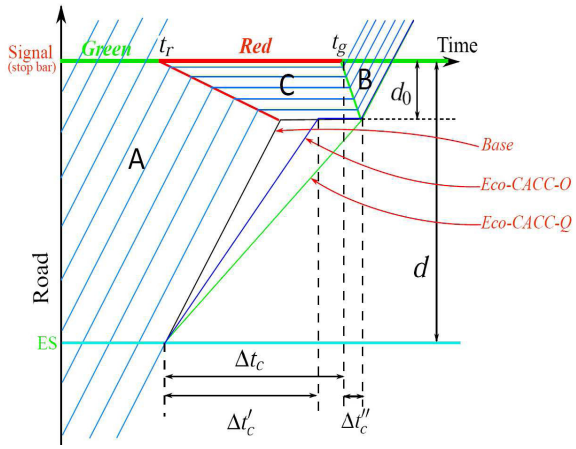

Fig. 2. Traffic dynamics at an intersection.

The model assumes that there exist a relationship between flow and density, i.e., the fundamental diagram,

$$q(x,t) = Q(\rho(x,t)); \tag{2}$$

Figure 1 illustrates a general fundamental diagram. Generally, the flow is a concave function of the density.

With green and red indications, traffic signals generate various shock waves and rarefaction waves, which lead to significant variations in vehicular movements. **Figure** 2 shows the movements of a series of vehicles approaching and passing an intersection with traffic waves. If one vehicle arrives at the intersection when the traffic signal indication is green, it proceeds through the intersection without any delay; while it has to wait at the stop bar for a green indication when the traffic signal indication is red. The red signal indication generates a shock wave upstream of the intersection.

Assume that the flow entering the intersection is q_0, and during the green indication, the traffic state upstream of the intersection is A, as shown in **Figure** 1. Once the signal turns red, no vehicles can proceed through the intersection, i.e., within the queue the traffic stream is at the maximum road density, ρ_j, and the discharge rate is reduced to 0. The upstream state becomes C, and a shock wave is generated and propagates backward. The speed of the shock wave is determined by the states A and C as

$$v_{AC} = \frac{q_0}{\rho_0 - \rho_j}. \tag{3}$$

Once the traffic signal turns green, the intersection starts to discharge vehicles at the saturation flow rate, i.e., q_c in **Figure** 1. As a result, a rarefaction wave is formed to release the queue upstream of the intersection, and the downstream state becomes B. The speed of the rarefaction wave is computed as

$$v_{CB} = \frac{q_c}{\rho_c - \rho_j}. \tag{4}$$

At time t, an Eco-CACC vehicle enters the control segment (travels a distance d from point ES to the traffic signal) with the speed v_0 ($v_0 = q_0/\rho_0$). Then, the tail location of the queue can be estimated as

$$d_0 = \begin{cases} \dfrac{v_{AC}}{v_0 + v_{AC}}[d - v_0(t_r - t)], \\ \qquad \forall t \in [t_r - \frac{d}{v_0}, t_g + \dfrac{v_{AC}(t_g - t_r)}{v_{AC} + v_{CB}}] \\ 0, \quad otherwise. \end{cases} \tag{5}$$

Here, t_r and t_r are the times that the traffic signal turns to a red and green indication, respectively. The stop duration of the vehicle ahead of the intersection is

$$t_{s,0} = \Delta t_c + \Delta t_c'' - \frac{d - d_0}{v_0}, \tag{6}$$

where $\Delta t_c = t_g - t$, and $\Delta t_c'' = \frac{d_0}{v_{CB}}$.

Note that if there are other Eco-CACC vehicles ahead, the propagation speed of the shock wave and the rarefaction wave cannot be estimated accurately using the fundamental diagram. Without vehicle-to-vehicle communication, the tail location cannot be identified exactly either. However, for the Eco-CACC vehicle, as it is controlled and does not pass any vehicles ahead, it considers all vehicles ahead as its queue. Hence, Eq(5) can still be applied to estimate the queue length with the assumption that all vehicles in the queue will stop at the traffic signal, which could result in an overestimation of the queue length.

In general, the speed of the rarefaction wave, v_{CB}, is greater than that of the shock wave, v_{AB}, as shown in **Figure** 1. As time progresses, the rarefaction wave will catch up with the shock wave and dissipate the queue. The traffic signal generates stop-and-go driving for individual vehicles, which increases fuel consumption levels significantly (see the base case in **Figure** 2). Consequently, controlling vehicle movements to ensure that they proceed through intersections smoothly without stopping is a critical factor in reducing vehicle fuel consumption levels.

III. Eco-CACC Algorithm Considering Queue Effects

In this section, an Eco-CACC algorithm is developed to improve an algorithm developed earlier in [22] with the consideration of vehicle queues and to further minimize the fuel consumption of vehicles proceeding through intersections. The mechanism of vehicle control in the algorithm is described as follows. Once an Eco-CACC vehicle enters the segment between the point *ES* and the traffic signal, which is defined as the upstream control segment of length d, as shown in **Figure** 2, the following two actions will be applied.

1) If the Eco-CACC vehicle can pass through the intersection at its original speed, v_0, without hitting the queue or the red indication, no control action will be applied to the vehicle, and the advisory speed limit is set as the free-flow speed, v_f.
2) If the vehicle cannot proceed through the intersection, we provide a lower speed limit, $v_c \leq v_0$, for the vehicle to approach the signal.

The basic criterion for estimating the advisory speed limit, v_c, is to reduce the stop duration while maintaining the average speed of the controlled vehicles without increasing their travel times. Reference [22] has demonstrated that the most critical strategy to reduce fuel consumption levels is to prevent vehicles from coming to a complete stop at the stop bar. However, without considering the impact of the queue, the strategy cannot prevent vehicle stops. Illustrated as the blue line (Eco-CACC-O) in **Figure** 2, the strategy proposed in [22] still forces vehicles to stop for the time $t_{s,1}$.

$$t_{s,1} = \Delta t_c - \Delta t_c' + \Delta t_c'', \tag{7}$$

where $\Delta t_c' = \frac{d-d_0}{v_2}$, and $v_2 = \frac{d}{\Delta t_c}$ is the advisory speed limit estimated by the Eco-CACC system without queue consideration (Eco-CACC-O). While considering the queue, the delay can be totally removed (see the green line (Eco-CACC-Q) in **Figure** 2).

In **Figure** 2, vehicles are controlled assuming infinite acceleration/deceleartion levels, which is not realistic. In this section, we develop an Eco-CACC algorithm considering queue effects (Eco-CACC-Q) to minimize vehicle vehicle fuel consumption levels while proceeding through an intersection with the consideration of realistic deceleration and acceleration levels, followed by an investigation of the impact of queue length on the algorithm performance.

A. Development of the Eco-CACC Algorithms

The Eco-CACC algorithms estimate time-dependent advisory speed limits considering realistic deceleration and acceleration levels to ensure that Eco-CACC vehicles decelerate to target speeds and cruise to the stop bar or the tail of the queue ahead of the intersection. Subsequently, once the queue is released, the probe vehicles accelerate to the free-flow speed at a constant throttle level. In that sense, the optimal deceleration and acceleration levels will be computed by the algorithms to minimize the total fuel consumed.

As shown in **Figure** 3(a), upstream of the intersection, the Eco-CACC-Q algorithm is activated for an Eco-CACC vehicle once it enters the control segment. Without control, the vehicle maintains its original speed v_0 until it stops at the end of the queue at the deceleration level, a_-^s. In the Eco-CACC algorithm without considering queue effects (Eco-CACC-O), the vehicle decelerates to a cruising speed, with which the vehicle cruises to the stop bar just when the signal turns green. While the queue forces the vehicle to stop at the queue tail at a deceleration level, a_-^s. Similarly, the Eco-CACC-Q algorithm reduces the speed of the probe vehicle at a constant deceleration level, however it allows the vehicle to arrive at the tail of the queue just when the queue is released, i.e., at $t = t_c$.

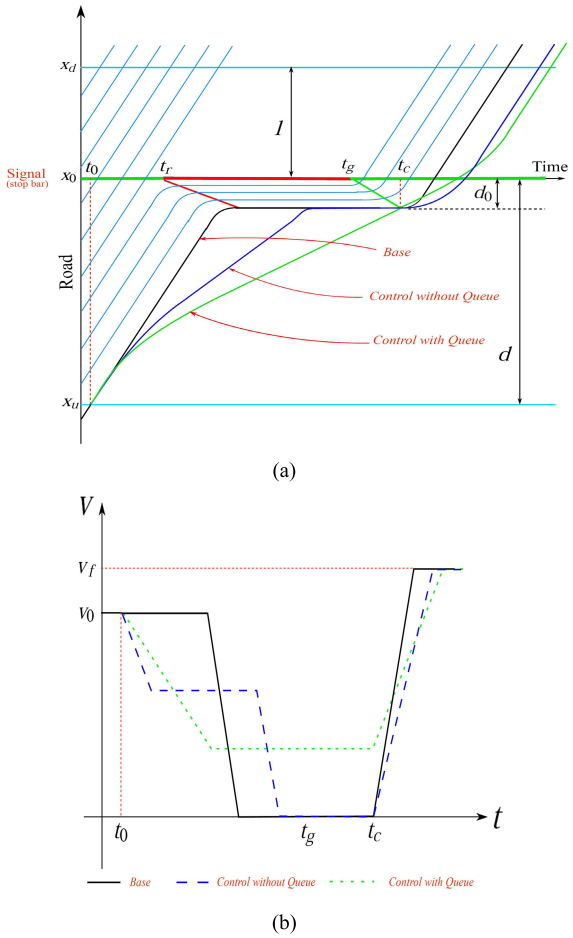

Fig. 3. Eco-CACC with deceleration and acceleration: (a) traffic dynamics at the intersection, (b) speed of the probe vehicle.

Downstream of the intersection, the algorithm should also allow the vehicle to accelerate back to the free-flow speed v_f at location x_d, where l is the length of the downstream control segment. Without control, the vehicle utilizes a constant acceleration level, a_+^s, to approach v_f. In the Eco-CACC-O and Eco-CACC-Q algorithms, optimal acceleration rates are applied for the vehicle to accelerate back to the free-flow speed at x_d. The acceleration levels are determined by the cruise speed and the distance x_d. The algorithms minimize the vehicle fuel consumption level by searching for the optimal combination of the upstream deceleration level, a_-, and the downstream acceleration level, a_+.

To develop Eco-CACC algorithms, the objective function is first defined in Eq(8). The algorithm is designed to minimize the total fuel consumed by Eco-CACC vehicles traversing the intersection.

$$\min_{a_-,a_+} \int_{t_0}^{t_0+T} F(v(t), v'(t))dt, \tag{8a}$$

$$s.t., \int_{t_0}^{t_0+T} v(t)dt = d + l. \tag{8b}$$

$$0 \leq a_- \leq a_-^s, \tag{8c}$$

$$0 \leq a_+ \leq a_+^s. \tag{8d}$$

$F(\cdot,\cdot)$ is a function of speed $v(t)$ and acceleration $v'(t)$, defined by the VT-CPFM model [37], to estimate the fuel consumption rate based on vehicular speed and acceleration levels.

$$F(v(t), v'(t)) = \begin{cases} \alpha_0 + \alpha_1 P(t) + \alpha_2 P^2(t) & P(t) \geq 0 \\ \alpha_0 & P(t) < 0, \end{cases} \tag{9a}$$

where, $\{\alpha_0, \alpha_1, \alpha_2\}$ are the coefficients determined by vehicle types. $P(t)$ is the vehicle power at time t, and it is a function of speed and acceleration.

$$P(t) = \frac{R(t) + m \cdot v'(t)(1.04 + 0.0025\xi^2(t))}{3600\eta_d} \cdot v(t), \tag{9b}$$

$$R(t) = \frac{\rho_a}{25.92} C_D C_h A_f v^2(t) + 9.8066 m \frac{C_r}{1000}(c_1 v(t) + c_2) + 9.8066 m G(t). \tag{9c}$$

Here, $R(t)$ is the resistance force of the vehicle, and $\xi(t)$ is the gear ratio, and $G(t)$ is the road grade at time t. $m, \rho_a, \eta_d, C_D, C_h, A_f$ represent the vehicle mass, the density of the air, the vehicle drag coefficient, the correction factor of altitude, and the vehicle front area, respectively. C_r, c_1, c_2 are rolling resistance parameters that vary as a function of the road surface type, road condition, and vehicle tire type.

In Eq(8a), $v(t)$ is the advisory speed limit of Eco-CACC vehicles traveling in the vicinity of the intersection at time t, computed using Eq(10) and Eq(11) for the Eco-CACC-O and Eco-CACC-Q algorithms, respectively. T is the time duration that the probe vehicle travels the upstream and downstream control segments. In the Eco-CACC-O algorithm the duration is defined as $T = T_n$; while, it is defined as $T = T_q$ for the Eco-CACC-Q algorithm.

For *Eco-CACC-O*, $v(t)$ can be computed as

$$v(t) = \begin{cases} v_0 - a_-(t - t_0), & t \in [t_0, t_0 + \delta t_{n,1}) \\ v_{n,t}, & t \in [t_0 + \delta t_{n,1}, t_0 + \delta t_{n,1} + \delta t_{n,2}) \\ v_{n,t} - a_-^s(t - t_0 - \delta t_{n,1}), & \\ \qquad t \in [t_0 + \delta t_{n,1} + \delta t_{n,2}, & \\ \qquad t_0 + \delta t_{n,1} + \delta t_{n,2} + \delta t_{n,3}) & \\ 0, & t \in [t_0 + \delta t_{n,1} + \delta t_{n,2} + \delta t_{n,3}, t_c) \\ v_{n,t} + a_+(t - t_c), & t \in [t_c, t_c + \delta t_{n,4}) \\ v_f, & t \in [t_c + \delta t_4, t_0 + T_n] \end{cases} \tag{10a}$$

Here, $v_{n,t}$ is defined as the algorithm cruise speed without considering the queue effects. The speed profile is shown as the blue dashed line in **Figure** 3(b). Furthermore, given the values of a_- and a_+, the variables, $\{T_n, v_{n,t}, \delta t_{n,1}, \delta t_{n,2}, \delta t_{n,3}, \delta t_{n,4}\}$ can be estimated using Eq(10)(b)-(g).

$$\delta t_{n,1} = \frac{v_0 - v_{n,t}}{a_-}, \tag{10b}$$

$$v_0 \cdot \delta t_{n,1} - \frac{1}{2} a_- \delta t_{n,1}^2 + v_{n,t}\delta t_{n,2} + v_{n,t}\delta t_{n,3} + \frac{1}{2} a_-^s \delta t_{n,3}^2 = d - d_0, \tag{10c}$$

$$v_0 \cdot \delta t_{n,1} - \frac{1}{2} a_- \delta t_{n,1}^2 + v_{n,t}\delta t_{n,2} + v_{n,t}(t_g - t_0 - \delta t_{n,1}) = d, \tag{10d}$$

$$\delta_{n,3} = \frac{v_{n,t}}{a_-^s}, \tag{10e}$$

$$\delta_{n,4} = \frac{v_f}{a_+}, \tag{10f}$$

$$\frac{1}{2} a_+ \delta t_{n,4}^2 + v_f \cdot (t_0 + T_n - t_c - \delta t_{n,4}) = l + d_0. \tag{10g}$$

For *Eco-CACC-Q*, there is

$$v(t) = \begin{cases} v_0 - a_-(t - t_0), & t \in [t_0, t_0 + \delta t_{q,1}) \\ v_{q,t}, & t \in [t_0 + \delta t_{q,1}, t_c) \\ v_{q,t} + a_+(t - t_c), & t \in [t_c, t_c + \delta t_{q,2}) \\ v_f, & t \in [t_c + \delta t_{q,2}, t_0 + T_q]. \end{cases} \tag{11a}$$

Here, $v_{q,t}$ is the cruise speed of the algorithm with queue. The speed profile is illustrated as the green dotted line in **Figure** 3(b). And, given the values of a_- and a_+, the variables, $\{T_q, v_{q,t}, \delta t_{q,1}, \delta t_{q,2}\}$ can be estimated by Eq(11)(b)-(e).

$$\delta t_{q,1} = \frac{v_0 - v_{q,t}}{a_-}, \tag{11b}$$

$$v_0 \cdot \delta t_{q,1} - \frac{1}{2} a_- \delta t_1^2 + v_{q,t}(t_c - t_0 - \delta t_{q,1}) = d - d_0, \tag{11c}$$

$$\delta t_{q,2} = \frac{v_f - v_{q,t}}{a_+}, \tag{11d}$$

$$v_t \cdot \delta t_{q,1} + \frac{1}{2} a_+ \delta t_{q,2}^2 + v_f \cdot (t_0 + T_q - t_c - \delta t_{q,2}) = l + d_0. \tag{11e}$$

Given the road traffic condition, including the queue length, start and end times of each phase, and the approaching speed of the probe vehicles, the speed profile is a function of a_- and a_+ (see Eq(10) and Eq(11)). Since the fuel consumption rate is determined by the speed profile, there exist the optimal deceleration and acceleration rates to minimize the fuel consumption rate. The Eco-CACC algorithms search for the optimal values within appropriate ranges (Eq(8)(c) and (d)).

The details of the Eco-CACC-Q algorithm is described below.

1) For a probe vehicle k, once it enters the segment $[x_u, x_d]$, where x_u and x_d are the start and end points of the control region, the algorithm is activated.
2) Upstream of the intersection
   a) The algorithm provides an advisory speed limit to the probe vehicles for the following two scenarios; otherwise, the free-flow speed is used as the advisory limit.
      i) The current signal indicator is green, but the traffic signal will turn red when the vehicle arrives at the stop bar if it travels at its current speed.
      ii) The current signal indicator is red and will continue to be red when the vehicle arrives at the stop bar while traveling at its current speed.

b) Once either of the above scenarios occurs, we predict the queue length ahead of the Eco-CACC vehicle, and estimate the release time of the queue, t_c, based on the speed of the rarefaction wave (see Eq(5)).
c) The algorithm estimates the optimal upstream deceleration level and the downstream acceleration level using Eq(8) and Eq(11) to minimize the vehicle fuel consumption, and provides an advisory speed limit to the Eco-CACC vehicle at the next time step $t + \Delta t$, where Δt is the speed update interval.

3) Downstream of the intersection, the algorithm searches for the optimal acceleration level based on its current speed to minimize the fuel consumption to reach the free-flow speed v_f at location x_d.
4) Once the Eco-CACC vehicle arrives at x_d, the Eco-CACC-Q algorithm is deactivated.

B. Impact of Queue Length

The impact of the queue length on the Eco-CACC-Q algorithm performance is investigated in this section. We apply an ideal simplistic example to analyze the impact of the queue length on the algorithm performance. Assume that the lengths of the controlled segments upstream and downstream of the intersection are $d = 500$ m, and $l = 200$ m, respectively. The Eco-CACC vehicle arrives at location x_u at $t_0 = 0$ s with an initial speed $v_0 = 72$ km/h, and the signal turns green at $t_g = 60$ s. Moreover, the free-flow speed, the roadway saturation flow rate, the jam density, and the density-at-capacity are $v_f = 72$ km/h, $q_c = 1600$ veh/h, $\rho_j = 160$ veh/km, and $\rho_c = 20$ veh/km,[1] respectively. Here, we assume that the Eco-CACC vehicle is a 2011 Honda Civil or similar; and the values of the parameters in the VT-CPFM model are calibrated in [37]

Figure 4 illustrates the impact of queue length on the total fuel consumed and the cruise speed. Generally, with the longer queue length, the advisory cruise speed is smaller. This is true, as a longer queue indicates the cruise distance is shorter, and the queue dissipation time is longer.[2] Moreover, both the Eco-CACC algorithms significantly reduce the fuel consumption of the Eco-CACC vehicles. The Eco-CACC-O algorithm reduces the fuel consumption by as high as 25% while the Eco-CACC-Q algorithm reduces the fuel consumption by 32%. Comparing the two algorithms, the Eco-CACC-Q algorithm produces fuel consumption levels that are 10% lower. Furthermore, with longer queues, the cruise speed is smaller, which can be derived from Eq(11). At the same time, the fuel consumption is larger. This finding demonstrates that the Eco-CACC-Q algorithm can further improve the fuel efficiency of Eco-CACC vehicles.

[1]These four variables are also applied to the Van Aerde model fundamental diagram [38].

[2]It is not exactly true that the advisory cruise speed is smaller for a longer queue (see the fluctuation in the curve in **Figure** 4(b)), as the upstream deceleration and downstream acceleration levels should be optimized to reduce the fuel consumption of Eco-CACC vehicles. Furthermore, a larger deceleration results in larger cruise speeds. Both acceleration and deceleration levels vary with queue lengths, and the cruise speed oscillates, as shown in **Figure** 4(b).

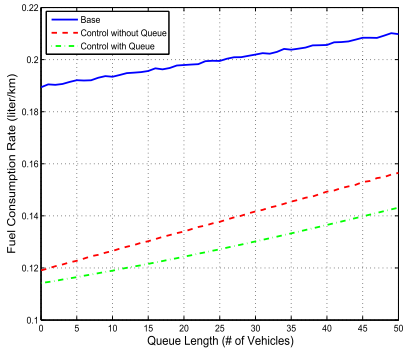

(a)

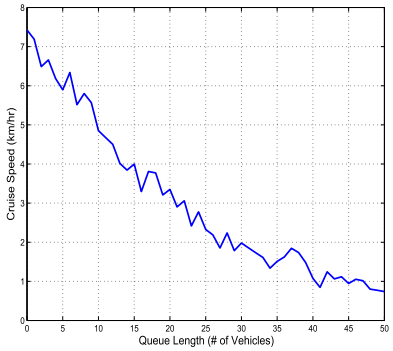

(b)

Fig. 4. Impact of queue length: (a) fuel consumption level, (b) Eco-CACC algorithm recommended speed.

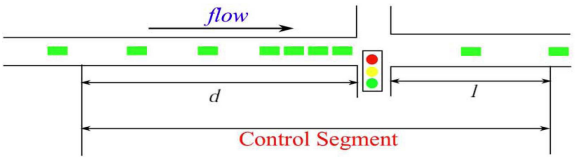

Fig. 5. Intersection Configuration.

IV. Case Studies

In this section, the Eco-CACC-Q algorithm is evaluated for different intersection configurations, as illustrated in **Figure** 5. We start with a single approach intersection (see **Figure** 5) with an upstream segment of length d and a downstream segment of length l. One- and two-lane roads are simulated using the INTEGRATION microscopic traffic simulator [39] to evaluate the Eco-CACC-Q algorithm performance. The INTEGRATION model uses the Rakha-Pasumarthy-Adjerid (RPA) car-following model to simulate the longitudinal vehicle motion [40]–[42]. In the RPA model the steady-state behavior is governed by the Van Aerde fundamental diagram [38], [43], which is also applied in this study to estimate the queue length ahead of the intersection. The simulator has been validated to model both microscopic and macroscopic traffic streams in the literature [44]–[47].

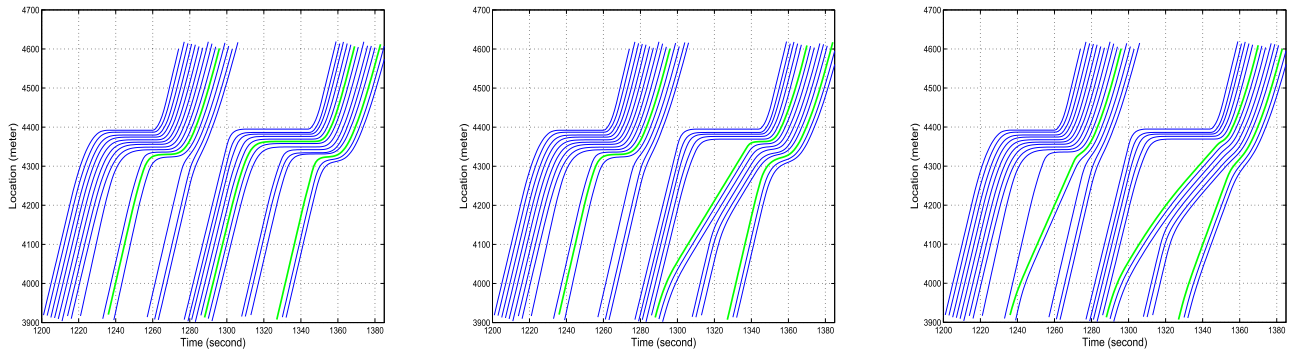

Fig. 6. Vehicle trajectories around a single-lane intersection: (a) base case, (b) Eco-CACC without queue, (c) Eco-CACC with queue.

A. Algorithm Performance on Single-Lane Roads

In this subsection, single-lane intersection approaches, where both the upstream and downstream roads have only one lane, are considered. This configuration ensures that all vehicles do not pass their leaders and that the Eco-CACC-Q algorithm is not affected by lane-changing behavior. In the simulation, the free-flow speed, the jam density, the saturation flow rate, and the speed-at-capacity are set as $v_f = 80$ km/h, $\rho_j = 160$ veh/km, $q_c = 1600$ veh/h, and $v_c = 60$ km/h, respectively. For the SPaT plan of the intersection, we set the green, amber, and red durations as 40 seconds, 4 seconds, and 40 seconds, respectively.

Assume that a constant demand of $q = 500$ veh/h is loaded to the intersection for one hour, and 20% of the vehicles act as Eco-CACC vehicles with equipped with wireless communication devices to receive the SPaT and vehicle queue information, i.e., approximately 100 CVs are loaded on the network. Here, we assume that all vehicles are the type 1 vehicle defined in VT-CPFM model. The length of the control segments upstream and downstream of the intersection are assumed to be $d = 500$ meters and $l = 200$ meters, respectively. All CVs apply both the Eco-CACC-O and Eco-CACC-Q algorithms, and the advisory speed limits are updated every second.[3]

Figure 6 illustrates the trajectories of all vehicles before and after applying the Eco-CACC algorithms at the intersection over two cycles, where the signal is located at $x = 4400$ meters. In **Figure** 6(a), without control, the Eco-CACC vehicles just follow their leaders, and they come to a complete stop ahead of the traffic signal waiting for the green indication to release the queue. **Figure** 6(b) shows the trajectories after applying the Eco-CACC-O algorithm. As can be seen from the second Eco-CACC vehicle in the figure, the vehicle slows down to approach the traffic signal and catches the green light. Because of the vehicle queue, the vehicle has to stop ahead of the intersection to wait for the release of the queue. While in **Figure** 6(c), the Eco-CACC-Q algorithm ensures that the vehicle is able to cruise to the intersection and catch the tail of the queue just when it is released, so that the vehicle can avoid coming to a complete stop upstream of the intersection.

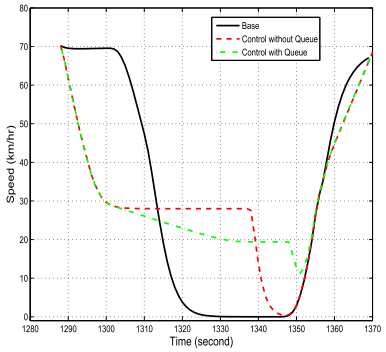

Fig. 7. Speed profiles of the second probe vehicle in the single-lane intersection.

Note that in **Figure** 6(b), the first and the third Eco-CACC vehicles are not controlled by the Eco-CACC algorithms. The reason is that the Eco-CACC-O algorithm estimates that the vehicles will proceed through the intersection at their current speed. However, due to the impact of the vehicle queues, the vehicles have to wait for the release of the queue. Hence, they still experience complete stops. The Eco-CACC-Q algorithm solves this problem. Consequently, we observe these two vehicles are controlled in **Figure** 6(c) and do not stop at the signal.

Figure 7 compare the the speed profiles of the second probe vehicle for the three different scenarios, respectively. The speed profiles computed by the Eco-CACC algorithms are much smoother than the base case, and the Eco-CACC-Q algorithm generates the smoothest trajectory (The standard deviations of the speed profiles from the base case, Eco-CACC-O, and Eco-CACC-Q are 29.7 km/h, 17.2 km/h, and 15.3 km/h, respectively.) Moreover, for the Eco-CACC-O algorithm, the probe vehicle cruises at a speed of 28 km/h, and stops for approximately 8 seconds (for the base case, it stops for approximately 30 seconds.).[4] While being controlled by the Eco-CACC-Q algorithm, the vehicle cruises at 20 km/h,

[3]The assumption is that the CACC system implements these speed recommendations without any intervention from the driver.

[4]The vehicle is considered stopped when its speed is less than that of a pedestrian, namely 1.2 m/s.

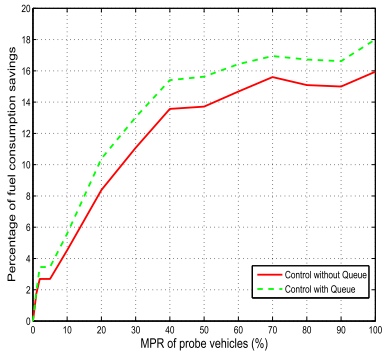

Fig. 8. Savings of fuel consumption rate for different MPRs on a single-lane intersection.

and does not stop upstream of the traffic signal. Furthermore, the fuel consumption generated by the probe vehicles are 0.125 l/km for the base case, 0.116 l/km for Eco-CACC-O, and 0.111 l/km for Eco-CACC-Q, respectively. In summary, the Eco-CACC-Q algorithm is the most efficient control strategy, with reductions in fuel consumption levels as high as 11.4%; and compared with Eco-CACC-O, it reduces fuel consumption levels by approximately 4.5%.

Besides the probe CVs, both Eco-CACC algorithms smooth the behavior of non-CVs given that they are governed by car-following rules and thus would have to follow the behavior of their lead vehicle (it should be noted that the approaches are single lanes). This means the algorithm is able to reduce the overall fuel consumption at the signalized intersection. The example above demonstrates that the algorithm without queue consideration and with queue consideration reduces the fuel consumption level by approximately 8.4% and 10.4%, respectively.

In addition, we investigate the impact of market penetration rates (MPRs) on the Eco-CACC algorithm performance. The settings of the simulation are the same as the example above, except that the MPR varies from 0 to 100%. **Figure** 8 shows the savings in the average fuel consumption derived from the algorithm with and without queue consideration. With higher MPRs, the fuel savings are higher. If all vehicles are controlled by the algorithm, the fuel consumption is reduced by approximately 15.9% for Eco-CACC-O, and 18.0% for Eco-CACC-Q. Thus, the algorithm considering the queue produces additional fuel savings.

B. Algorithm Performance on Multi-Lane Roads

In this subsection, a simulation for a more realistic intersection layout, namely a multi-lane intersection where the roads upstream and downstream of the intersection have more than a single lane, is considered. To simplify the simulation, we simulate a two-lane intersection. The scenario is designed to quantify the benefits of the algorithm for different MPRs with realistic network topologies. The settings of the roads, the signal phasing and timing plan, the vehicle type, and the Eco-CACC algorithm are the same as the simulation configuration that was described in the previous subsection. In that sense, the lane-based fundamental diagram remains the same. The demand entering the intersection is set as $q = 500$ veh/h/lane, i.e., 1000 veh/h. Vehicles are loaded to the network for approximately one hour. We assume 20% of vehicles are CVs that receive SPaT and vehicle queue information.

Figure 9 illustrates the vehicle trajectories for vehicles on the left lane before and after applying the Eco-CACC algorithm over two cycle lengths, where the signal is located at $x = 4400$ meters. Without control, the probe vehicles in **Figure** 9(a) only follow their leaders. In **Figure** 9(b), the probe vehicles are controlled by the Eco-CACC-O algorithm, and thus cannot avoid incurring a complete stop. In **Figure** 9(c), the probe vehicles are controlled by the Eco-CACC-Q algorithm to allow the vehicles to proceed through the intersection without incurring a stop.

Figure 10 compares the speed profiles of the first CV (the second one in **Figure** 9(a)) for the three scenarios, respectively. It demonstrates that the Eco-CACC-Q algorithm generates the smoothest speed profile (the standard deviations of the speed from the base case, Eco-CACC-O, and Eco-CACC-Q are 31.9 km/h, 19.2 km/h, 16.5 km/h, respectively). For the Eco-CACC-O algorithm, the CV cruises at a speed of 40 km/h, and experiences a stop of approximately 6 seconds (for the base case, it stops for approximately 17 seconds). While when the Eco-CACC-O algorithm is used, the vehicle cruises at 20 km/h, and does not stop upstream of the traffic signal.[5] The fuel consumption rates generated by the probe vehicles are 0.125 l/km for the base case, 0.107 l/km for Eco-CACC-O, and 0.101 l/km for Eco-CACC-Q, respectively. In summary, the Eco-CACC-Q algorithm provides the most efficient control, with reductions in fuel consumption levels for CVs as high as 19.2%; and compared with Eco-CACC-O, it reduces fuel consumption levels by approximately 5.6%.

Unlike the example in the previous subsection, both roads have two lanes. Consequently, as the CVs are controlled and travel at a lower speed compared to the surrounding traffic, non-CVs make lane changes to cut into the gaps ahead of the CVs (see **Figure** 9). The overall average speed of the CVs is further reduced, i.e., they take longer time to reach the same position downstream of the intersection (see **Figure** 10(a)). Moreover, another drawback of the algorithm is that the intense lane changing behavior, which cause frequent accelerations and traffic oscillations, result in high fuel consumption levels for low MPRs. In that sense, the overall fuel consumption may increase. Below MPRs of 20% both the Eco-CACC-O and Eco-CACC-Q algorithm result in an increase in the fuel consumption level by approximately 5%.

Moreover, we investigate the impact of MPRs on the Eco-CACC algorithm performance. The settings of the simulation are the same as the example above, except that the MPR varies from 0 to 100%. **Figure** 11 shows the savings in the average fuel consumption rate for all vehicles for the two algorithms. For lower MPRs, both algorithms have a negative impact on the overall fuel consumption rate. This is caused by the intense lane changes around the controlled vehicles. Once the MPR is greater than 30%, the number

[5]Due to lane-changing behavior, the queue length changes over time and thus the recommended cruise speed also changes over time.

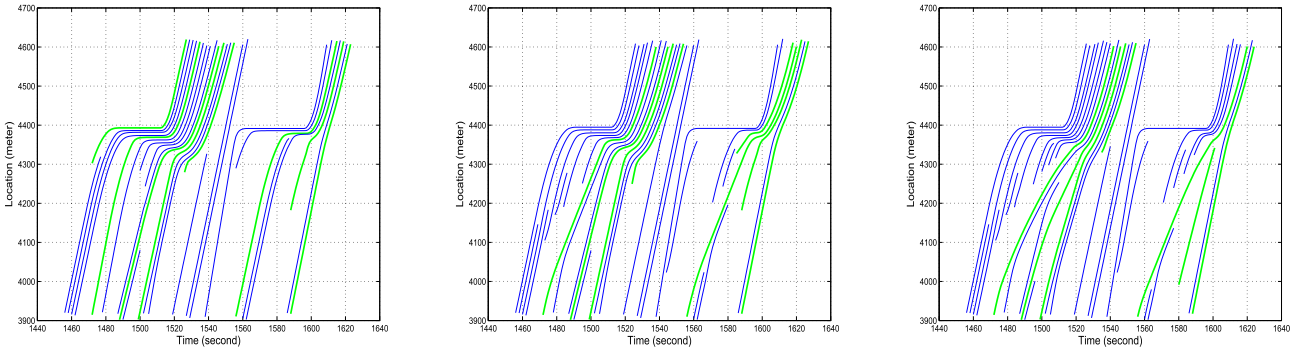

Fig. 9. Vehicle trajectories around the intersection: (a) base case, (b) Eco-CACC without queue, (c) Eco-CACC with queue.

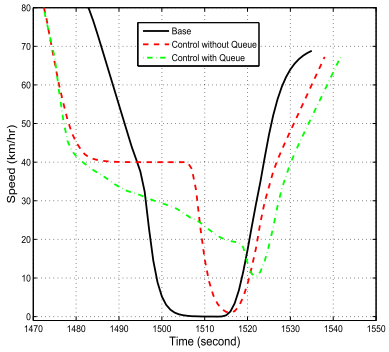

Fig. 10. Speed profiles of the second probe vehicle in the two-lane intersection.

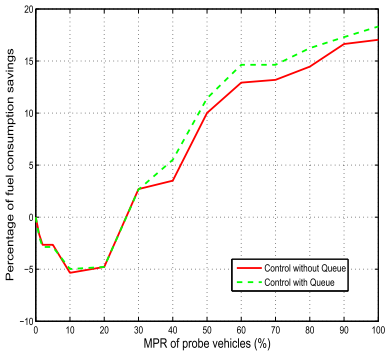

Fig. 11. Savings of fuel consumption rate for different MPRs on a multi-lane intersection.

of Eco-CACC vehicles is large enough to prevent the non-Eco-CACC vehicles from cutting in and thus reduce the lane change intensity. Hence, the Eco-CACC algorithms generate generate fuel consumption savings at higher MPRs. These savings increase as the MPR increases. If all vehicles are Eco-CACC vehicles, the fuel consumption rate is reduced by approximately 17.0% for Eco-CACC-O, and 18.3% for Eco-CACC-Q demonstrating the benfits of the Eco-CACC-Q system.

V. Conclusions

This paper developed an Eco-CACC-Q algorithm to minimize fuel consumption levels of vehicles proceeding through signalized intersections. The algorithm utilizes SPaT information accessed through V2I and V2V communications and predicted vehicle queues derived from road-side loop detectors to compute optimum instantaneous vehicle speeds. The algorithm predicts the length of the queue ahead of the probe vehicles using the LWR model and predicts the release time of the queue using the SPaT information. A second-by-second advisory speed limit is provided to the CVs to reduce the number of stops and the optimal upstream deceleration and downstream acceleration level are estimated to minimize fuel consumption levels. The analysis of the proposed algorithm indicated that longer vehicle queue lengths resulted in higher fuel consumption levels, but both the Eco-CACC-O and Eco-CACC-Q algorithms produced reductions in fuel consumption levels. However, the Eco-CACC-Q algorithm produced larger reductions in fuel consumption levels.

Besides the analytical work, the algorithm was also tested using the INTEGRATION microscopic traffic simulation software. The simulation of a single-lane intersection indicated that both the Eco-CACC-O and Eco-CACC-Q algorithms produced smoother vehicle trajectories. The queue prediction enhanced the Eco-CACC-Q algorithm to produce the smoothest vehicle trajectories and to result in the highest fuel savings, approximately 11.4%. Moreover, with higher MPRs, the savings increased. At an MPR of 100% fuel savings of approximately 18.0% were achievable. For multi-lane intersections, the algorithm was still able to reduce the fuel consumption level of probe vehicles by approximately 19.2%. However, for MPRs less than 30%, the slower CVs produced intense lane changes in the gaps they left ahead of them and thus produced increased overall fuel consumption levels. Only when the MPRs were greater than 30%, the Eco-CACC system produced positive fuel savings. For MPRs of 100%, fuel savings of 17.0% and 18.3% were achieved for Eco-CACC-O and Eco-CACC-Q, respectively.

The analysis presented in the paper only investigated the impact of MPRs on the algorithm performance. Other factors that should be considered include length of the controlled segments, traffic demand levels, and SPaT plan. Consequently, a comprehensive sensitivity analysis of these factors on the algorithm performance is needed. Also, the robustness of

the algorithm to errors in wireless communication and driver responses should be analyzed. Moreover, further improvements to the proposed Eco-CACC-Q algorithm may be made by considering multiple signalized intersections in the optimization logic. Furthermore, the proposed algorithm only applied vehicle-to-signal communications to gather road traffic information, which was not sufficient to estimate the queue length accurately due to lane-changing and passing behavior. In the future, we will introduce vehicle-to-vehicles communications to queue length estimation algorithm [48]. Finally, one drawback of the algorithm is that it fails once the road is over-saturated. Hence, we propose that we combine a speed harmonization algorithm [49] on arterial roads and signal optimization with the Eco-CACC-Q algorithm to solve this problem and to further improve the system benefits.

REFERENCES

[1] C2ES. *Transporation Overview*, accessed on Oct. 25, 2015. [Online]. Available: http://www.c2es.org/

[2] N. Jollands *et al.*, "The 25 IEA energy efficiency policy recommendations to the g8 gleneagles plan of action," *Energy policy*, vol. 38, no. 11, pp. 6409–6418, 2010.

[3] J. N. Barkenbus, "ECO-driving: An overlooked climate change initiative," *Energy Policy*, vol. 38, no. 2, pp. 762–769, 2010.

[4] H. Rakha, K. Ahn, and A. Trani, "Comparison of MOBILE5a, MOBILE6, VT-MICRO, and CMEM models for estimating hot-stabilized light-duty gasoline vehicle emissions," *Can. J. Civil Eng.*, vol. 30, no. 6, pp. 1010–1021, 2003.

[5] M. Barth and K. Boriboonsomsin, "Real-world carbon dioxide impacts of traffic congestion," *Transp. Res. Rec.*, vol. 2058, no. 1, pp. 163–171, 2008.

[6] Y. Ding and H. Rakha, "Trip-based explanatory variables for estimating vehicle fuel consumption and emission rates," *Water Air Soil Pollution, Focus*, vol. 2, nos. 5–6, pp. 61–77, 2002.

[7] M. Barth and K. Boriboonsomsin, "Energy and emissions impacts of a freeway-based dynamic ECO-driving system," *Transp. Res. Part D, Transp. Environ.*, vol. 14, no. 6, pp. 400–410, 2009.

[8] H. Yang and W.-L. Jin, "A control theoretic formulation of green driving strategies based on inter-vehicle communications," *Transp. Res. C, Emerg. Technol.*, vol. 41, pp. 48–60, Apr. 2014.

[9] S. Park, H. Rakha, K. Ahn, K. Moran, B. Saerens, and E. Van den Bulck, "Predictive ECO-cruise control: Algorithm and potential benefits," in *Proc. IEEE Forum Integr. Sustain. Transp. Syst. (FISTS)*, Jun./Jul. 2011, pp. 394–399.

[10] S. Park, H. A. Rakha, K. Ahn, K. Moran, B. Saerens, and E. Van den Bulck, "Predictive Eco-cruise control system: Model logic and preliminary testing," *Transp. Res. Rec.*, vol. 2270, no. 1, pp. 113–123, 2012.

[11] K. Ahn, H. Rakha, and S. Park, "ECOdrive application: Algorithmic development and preliminary testing," *Transp. Res. Rec.*, vol. 2341, no. 1, pp. 1–11, Feb. 2013.

[12] X. Li, G. Li, S.-S. Pang, X. Yang, and J. Tian, "Signal timing of intersections using integrated optimization of traffic quality, emissions and fuel consumption: A note," *Transp. Res. D*, vol. 9, no. 5, pp. 401–407, 2004.

[13] A. Stevanovic, J. Stevanovic, K. Zhang, and S. Batterman, "Optimizing traffic control to reduce fuel consumption and vehicular emissions," *Transp. Res. Rec.*, vol. 2128, no. 1, pp. 105–113, 2009.

[14] U.S. Department of Transportation. (2015). *Connected Vehicle Research in the United States*, accessed on Oct. 25, 2015. [Online]. Available: http://www.its.dot.gov/connected_vehicle/

[15] S. Mandava, K. Boriboonsomsin, and M. Barth, "Arterial velocity planning based on traffic signal information under light traffic conditions," in *Proc. 12th Int. IEEE Conf. Intell. Transp. Syst.*, Oct. 2009, pp. 1–6.

[16] H. Xia, K. Boriboonsomsin, and M. Barth, "Dynamic ECO-driving for signalized arterial corridors and its indirect network-wide energy/emissions benefits," *J. Intell. Transp. Syst.*, vol. 17, no. 1, pp. 31–41, 2013.

[17] B. Asadi and A. Vahidi, "Predictive cruise control: Utilizing upcoming traffic signal information for improving fuel ECOnomy and reducing trip time," *IEEE Trans. Control Syst. Technol.*, vol. 19, no. 3, pp. 707–714, May 2011.

[18] K. J. Malakorn and B. Park, "Assessment of mobility, energy, and environment impacts of intellidrive-based cooperative adaptive cruise control and intelligent traffic signal control," in *Proc. IEEE Int. Symp. Sustain. Syst. Technol.(ISSST)*, May 2010, pp. 1–6.

[19] M. Barth, S. Mandava, K. Boriboonsomsin, and H. Xia, "Dynamic ECO-driving for arterial corridors," in *Proc. IEEE Forum Integr. Sustain. Transp. Syst. (FISTS)*, Jul. 2011, pp. 182–188.

[20] H. Rakha and R. K. Kamalanathsharma, "ECO-driving at signalized intersections using V2I communication," in *Proc. 14th Int. IEEE Conf. Intell. Transp. Syst. (ITSC)*, Oct. 2011, pp. 341–346.

[21] R. K. Kamalanathsharma and H. A. Rakha, "Multi-stage dynamic programming algorithm for ECO-speed control at traffic signalized intersections," in *Proc. 16th Int. IEEE Conf. Intell. Transp. Syst.-(ITSC)*, Oct. 2013, pp. 2094–2099.

[22] R. K. Kamalanathsharma, H. A. Rakha, and H. Yang, "Network-wide impacts of vehicle eco-speed control in the vicinity of traffic signalized intersections," *Transp. Res. Rec.*, vol. 2503, no. 1, pp. 91–99, 2015.

[23] G. De Nunzio, C. C. de Wit, P. Moulin, and D. Di Domenico, "ECO-driving in urban traffic networks using traffic signal information," in *Proc. 52nd IEEE Annu. Conf. Decision Control (CDC)*, Dec. 2013, pp. 892–898.

[24] K. Katsaros, R. Kernchen, M. Dianati, and D. Rieck, "Performance study of a green light optimized speed advisory (GLOSA) application using an integrated cooperative its simulation platform," in *Proc. IEEE 7th Int. Wireless Commun. Mobile Comput. Conf. (IWCMC)*, Jul. 2011, pp. 918–923.

[25] K. Katsaros, R. Kernchen, M. Dianati, D. Rieck, and C. Zinoviou, "Application of vehicular communications for improving the efficiency of traffic in urban areas," *Wireless Commun. Mobile Comput.*, vol. 11, no. 12, pp. 1657–1667, 2011.

[26] M. Seredynski, W. Mazurczyk, and D. Khadraoui, "Multi-segment green light optimal speed advisory," in *Proc. IEEE 27th Int. Parallel Distrib. Process. Symp. Workshops (IPDPSW)*, May 2013, pp. 459–465.

[27] M. Seredynski, B. Dorronsoro, and D. Khadraoui, "Comparison of green light optimal speed advisory approaches," in *Proc. 16th Int. IEEE Conf. Intell. Transp. Syst. (ITSC)*, Oct. 2013, pp. 2187–2192.

[28] ERTICO-ITS Europe. (2015). *ECOmove: Cooperative Mobility Systems and Service for Energy Efficiency*, accessed on Oct. 25, 2015. [Online]. Available: http://www.ECOmove-project.eu/

[29] E. Koukoumidis, L.-S. Peh, and M. R. Martonosi, "Signalguru: Leveraging mobile phones for collaborative traffic signal schedule advisory," in *Proc. 9th Int. Conf. Mobile Syst., Appl. Services ACM*, 2011, pp. 127–140.

[30] M. Munoz-Organero and V. C. Magana, "Validating the impact on reducing fuel consumption by using an ECOdriving assistant based on traffic sign detection and optimal deceleration patterns," *IEEE Trans. Intell. Transp. Syst.*, vol. 14, no. 2, pp. 1023–1028, Jun. 2013.

[31] G. Qian and E. Chung, "Evaluating effects of ECO-driving at traffic intersections based on traffic micro-simulation," in *Proc. 34th Autral. Transp. Res. Forum (ATRF)*, Adelaide, SA, Australia, 2011, vol. 34. no. 0092, pp. 1–11.

[32] G. Qian, "Effectiveness of ECO-driving during queue discharge at urban signalized intersections," Ph.D. dissertation, School Civil Eng. Build Environ., Queensland Univ. Technol., Brisbane City, QLD, Australia, 2013.

[33] Z. Chen, "An optimization model for ECO-driving at signalized intersection," Ph.D. dissertation, Zachry Dept. Civil Eng., Texas A&M Univ., College Station, TX, USA, 2013.

[34] Q. Jin, G. Wu, K. Boriboonsomsin, and M. J. Barth, "Power-based optimal longitudinal control for a connected ECO-driving system," *IEEE Trans. Intell. Transp. Syst.*, 2016, pp. 1–11.

[35] M. J. Lighthill and G. B. Whitham, "On kinematic waves. II. A theory of traffic flow on long crowded roads," *Proc. Roy. Soc. London, Ser. A, Math. Phys. Sci.*, vol. 229, no. 1178, pp. 317–345, 1955.

[36] P. I. Richards, "Shock waves on the highway," *Oper. Res.*, vol. 4, no. 1, pp. 42–51, 1956.

[37] H. A. Rakha, K. Ahn, K. Moran, B. Saerens, and E. Van den Bulck, "Virginia tech comprehensive power-based fuel consumption model: Model development and testing," *Transp. Res. D, Transp. Environ.*, vol. 16, no. 7, pp. 492–503, 2011.

[38] M. Van Aerde, "Single regime speed-flow-density relationship for congested and uncongested highways," in *Proc. 74th Annu. Meeting Transp. Res. Board*, vol. 6. Washington, DC, USA, 1995, no. 950802.
[39] H. Rakha, "INTEGRATION release 2.40 for Windows: User's guide," M. Van Aerde Assoc., Ltd., Blacksburg, VA, USA, Tech. Rep., 2013.
[40] H. Rakha, P. Pasumarthy, and S. Adjerid, "A simplified behavioral vehicle longitudinal motion model," *Transp. Lett.*, vol. 1, no. 2, pp. 95–110, 2009.
[41] H. Rakha, "Validation of van aerde's simplified steadystate car-following and traffic stream model," *Transp. Lett.*, vol. 1, no. 3, pp. 227–244, 2013.
[42] J. Sangster and H. Rakha, "Enhancing and calibrating the rakha-pasumarthy-adjerid car-following model using naturalistic driving data," *Int. J. Transp. Sci. Technol.*, vol. 3, no. 3, pp. 229–248, 2014.
[43] M. Van Aerde and H. Rakha, "Multivariate calibration of single regime speed-flow-density relationships [road traffic management]," in *Proc. 6th Veh. Navigat. Inf. Syst. Conf.*, vol. 334. Jul./Aug. 1995, pp. 334–341.
[44] H. Rakha, I. Lucic, S. H. Demarchi, J. R. Setti, and M. V. Aerde, "Vehicle dynamics model for predicting maximum truck acceleration levels," *J. Transp. Eng.*, vol. 127, no. 5, pp. 418–425, 2001.
[45] H. Rakha and I. Lucic, "Variable power vehicle dynamics model for estimating truck accelerations," *J. Transp. Eng.*, vol. 128, no. 5, pp. 412–419, 2002.
[46] H. Rakha and B. Crowther, "Comparison of greenshields, pipes, and Van Aerde car-following and traffic stream models," *Transp. Res. Rec., J. Transp. Res. Board*, no. 1802, no. 1, pp. 248–262, 2002.
[47] H. Rakha, M. Snare, and F. Dion, "Vehicle dynamics model for estimating maximum light-duty vehicle acceleration levels," *Transp. Res. Rec. J. Transp. Res. Board*, vol. 1883, no. 1, pp. 40–49, 2004.
[48] B. E. Badillo, H. Rakha, T. W. Rioux, and M. Abrams, "Queue length estimation using conventional vehicle detector and probe vehicle data," in *Proc. 15th Int. IEEE Conf. Intell. Transp. Syst. (ITSC)*, Sep. 2012, pp. 1674–1681.
[49] H. Yang and H. Rakha, "Developemnt of a speed harmonization algorithm: Methodology and preliminary testing," *Transp. Res. C*, submitted.

Hao Yang received the B.S. degree in automation from the University of Science and Technology of China, China, in 2008, and the M.S. and Ph.D. degrees in civil and environmental engineering from the University of California at Irvine, Irvine, CA, USA. He was a Post-Doctoral Associate with the Virginia Tech Transportation Institute, Blacksburg, VA, USA. He is currently a Visiting Assistant Professor with Lamar University, Beaumont, TX, USA. His research interests include intelligent transportation systems, connected and autonomous vehicles, environmental sustainability, traffic simulations, and transportation data analysis.

Hesham Rakha (M'04) received the B.Sc. degree (Hons.) in civil engineering from Cairo University, Cairo, Egypt, in 1987, and the M.Sc. and Ph.D. degrees in civil and environmental engineering from Queens University, Kingston, ON, Canada, in 1990 and 1993, respectively. He is currently the Samuel Reynolds Pritchard Professor of Engineering with the Charles E. Via, Jr. Department of Civil and Environmental Engineering, a Courtesy Professor with the Bradley Department of Electrical and Computer Engineering, and the Director of the Center for Sustainable Mobility with the Virginia Tech Transportation Institute. He is also a Professional Engineer in Ontario and a Member of the Institute of Transportation Engineers, the American Society of Civil Engineers, and the Transportation Research Board. He serves on the Editorial Board of the *Transportation Letters*, the IET *Intelligent Transport Systems Journal*, and the *International Journal of Transportation Science and Technology*. In addition, he is an Associate Editor for the IEEE TRANSACTIONS OF INTELLIGENT TRANSPORTATION SYSTEMS and the IEEE JOURNAL OF INTELLIGENT TRANSPORTATION SYSTEMS. His areas of research include traffic flow theory, traveler and driver behavior modeling, dynamic traffic assignment, transportation network control, use of artificial intelligence in transportation, intelligent vehicle systems, connected and automated vehicles, transportation energy and environmental modeling, and transportation safety modeling.

Mani Venkat Ala received the B.S. degree in civil engineering from IIT Guwahati, Guwahati, India, in 2012, and the M.S. degree in civil and environmental engineering from the Virginia Polytechnic Institute and State University, Blacksburg, VA, USA. He is currently a Research Engineer with KLD and Associates, Ltd. His current research interests include connected and autonomous vehicles, environmental sustainability, and traffic signal control.